

Phase measurements in open and closed Aharonov-Bohm interferometers

Amnon Aharony ^{a,1}, Ora Entin-Wohlman ^a and Yoseph Imry ^b

^a*School of Physics and Astronomy, Sackler Faculty of Exact Sciences, Tel Aviv University, tel Aviv 69978,*

Department of Physics, Ben-Gurion University, Beer Sheva 84105, Israel,

and Argonne National laboratory, Argonne, IL60439, USA

^b*Department of Condensed Matter Physics, Weizmann Institute of Science, Rehovot 76100, Israel*

Abstract

Mesoscopic Aharonov-Bohm interferometers have been used in attempts to measure the transmission phase of a quantum dot which is placed on one arm of the interferometer. Here we review theoretical results for the conductance through such interferometers, for both the closed (two-terminal) and open (multi-terminal) cases. In addition to earlier results for the Coulomb blockade regime, we present new results for the strongly correlated Kondo regime, and test the consistency of the two-slit analysis of some data from open interferometer experiments.

Key words: interference in nanostructures, Aharonov-Bohm interferometer, quantum dots, Kondo effect

PACS: , 73.21.-b, 71.27.+a, 03.75.-b, 85.35.Ds

1. Introduction and Review of Experiments

Mesoscopic quantum dots (QDs) represent artificial atoms with experimentally controllable properties [1,2,3]. Connecting a QD via two one-dimensional (1D) ‘metallic’ leads to electron reservoirs, one can vary the attraction of electrons to the QD by the ‘plunger gate voltage’, V_G . Measurements of the conductance \mathbf{G} through the QD, as function of V_G , show peaks whenever the Fermi energy ϵ_F of the electrons crosses a resonance on the QD. The quantum information on the resonant tunnelling through the QD is contained in the *complex* transmission amplitude, $t_{QD} = -i\sqrt{\mathbf{T}_{QD}}e^{i\alpha_{QD}}$. It is thus of great interest to measure the V_G -dependence of both the magnitude \mathbf{T}_{QD} and the phase α_{QD} .

The “textbook” method to measure the phase of a wave is based on the *two-slit interferometer* [4]. In this geometry, a coherent electron beam is split between two paths, going through two slits, and one measures the distribution of electrons absorbed on a screen behind the two slits. This distribution contains information on the relative phases of the electron wave functions in the two paths, via interference. In the Aharonov-Bohm interferometer (ABI) [5], one adds a magnetic flux Φ through the area between the two paths. This adds the Aharonov-Bohm phase difference $\phi = e\Phi/\hbar c$ between the phases of the wave functions in the two branches of the ring [6]. Denoting the “bare” transmission amplitudes through each path by $t_i = |t_i|e^{i\alpha_i}$, the “standard” two-slit formula for the outgoing electron distribution, or equivalently for the transmission through the ABI, has the form

$$\mathbf{T} = |t_1 e^{i\phi} + t_2|^2 = A + B \cos(\phi + \beta), \quad (1)$$

¹ Corresponding author. E-mail: aharony@post.tau.ac.il

with $\beta = \alpha_1 - \alpha_2$ and

$$A = |t_1|^2 + |t_2|^2, \quad B = 2|t_1||t_2|. \quad (2)$$

However, as discussed below, this formula applies only under very specific conditions.

Placing a QD on one path, and changing its plunger gate voltage V_G , would vary the corresponding amplitude $t_1 \equiv t_{QD}$. If the 2-slit formula were valid, it would allow the determination of the dependence of α_{QD} on V_G . This was the motivation of Yacoby *et al.* [7], who used a **closed mesoscopic ABI**, where a ring made of the two paths was connected to two terminals leading to two electron reservoirs. Indeed, the measured conductance was periodic in ϕ , and the detailed dependence of \mathbf{T} on ϕ varied with V_G , showing resonances. However, close to a resonance the data did not fit the simple 2-slit formula; they required more harmonics in ϕ . The data also exhibited “phase rigidity”: the fitted phase β did not follow the continuous variation with V_G (as would be implied from the 2-slit scenario, where $\beta = \alpha_{QD} + \text{const}$). Instead, β exhibited discrete jumps by $\pm\pi$ as V_G passes through each resonance.

This “phase rigidity” results from the Onsager relations. Unlike the 2-slit geometry, the closed ABI requires many reflections of the electron waves from the ‘forks’ connecting the ring with the leads. Each such reflection adds a term to the interference sum of amplitudes, and modifies the simple 2-slit formula. In fact, unitarity (conservation of current) and time reversal symmetry imply that the conductance \mathbf{G} (and therefore also the transmission \mathbf{T}) obey the symmetry $\mathbf{G}(\phi) = \mathbf{G}(-\phi)$ [8,9], and therefore β *must* be equal to 0 or π . As discussed below, the additional reflections also explain the need for higher harmonics near resonances.

Later experiments [10] used an **open interferometer**, by adding ‘lossy’ channels which break unitarity. Indeed, fitting the conductance to Eq. (1) yielded a phase $\beta(V_G)$ which was interpreted as representing the ‘intrinsic’ $\alpha_{QD}(V_G)$. Below we discuss the applicability of the two-slit formula to such experiments [11].

In all these experiments, one is restricted to small mesoscopic systems and to low temperatures, in order to maintain the coherence of the wave functions and observe quantum interference [2]. The above experiments were performed at relatively high temperatures, where the main effect of the Coulomb interac-

tions arises via Coulomb blockade, which introduces a separate resonance whenever V_G allows the addition of one more electron to the QD. As the temperature T decreases below the Kondo temperature T_K , and the QD is occupied by an odd number of electrons, the spin of these electrons is dynamically screened by the electrons in the Fermi sea, yielding a large conductance \mathbf{G} through the QD, close to the unitarity value $2e^2/h$, and a transmission phase α_{QD} equal to $\pi/2$ [12]. Aiming to test these predictions then led to experiments using the ABI at very low T , for both a closed (“two-terminal”) ABI [13] and an open (“multi-terminal”) ABI [14]. Both experiments exhibited the Aharonov-Bohm oscillations with ϕ . The former experiments exhibited the expected “phase rigidity”, but there has been no quantitative analysis of these data. The latter experiments used the two-slit formula to “measure” the transmission phase β , and found an unexpected variety of behaviors which were inconsistent with the theoretical value $\alpha_{QD} = \pi/2$.

During the last few years we obtained several theoretical results concerning the interpretation of the above experiments. Below we review some of these earlier results, and report on some recent new results.

2. Model for the ABI

All our calculations are done for the model shown in Fig. 1. The conductance \mathbf{G} is measured between the two leads which are attached to sites “L” and “R” on the ABI ring. The QD (denoted “D”) is on the upper branch, and is connected to L (R) via n_l (n_r) sites. The lower “reference” branch contains n_0 sites. Except for the QD, we use a tight binding model, with the real hopping matrix elements as indicated in the figure, and with site energies ϵ_l , ϵ_r and ϵ_0 on the respective branches, and ϵ_L , ϵ_R on sites L and R. The site energies on the leads are set at 0. The normalized flux ϕ is introduced as a phase factor in $J_{D1} = J_{1D}^* = jie^{i\phi}$ (gauge invariance allows placing it on any bond(s) around the ring). Assuming that the transmission is dominated by a single resonance on the QD, the Hamiltonian on the dot is assumed to have the form

$$\mathbf{H}_d = \epsilon_d \sum_{\sigma} n_{d\sigma} + U n_{d\uparrow} n_{d\downarrow}, \quad (3)$$

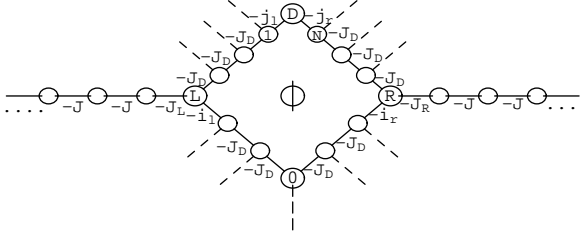


Fig. 1. Model for the ABI.

with $n_{d\sigma} = d_\sigma^\dagger d_\sigma$ being the number operator for an electron with spin σ on the QD. We also assume that U is very large, and ignore the resonance at $2\epsilon_d + U$. For the open ABI, each dashed line represents an additional lead, with a hopping matrix element $-J_X$ on its first bond [11].

In the absence of the lower “reference” branch, and when $J_L = J_D = J_R = J$, $\epsilon_L = \epsilon_R = \epsilon_l = \epsilon_r = 0$, the transmission amplitude through the upper branch reduces to [15]

$$\begin{aligned} t_{QD} &= -i\gamma_D \sin \alpha_{QD} e^{i\alpha_{QD}} \\ &= 2i \sin |ka| j_l j_r G_{up}(\epsilon_k) / J, \end{aligned} \quad (4)$$

where $\epsilon_k = -2J \cos(ka)$ is the energy of the electron in the band (equal to the Fermi energy), and G_{up} is the retarded Green function of an electron on the QD for this geometry. Here, $\gamma_D = 2j_l j_r / (j_l^2 + j_r^2)$. If these one-dimensional conditions apply, then this equation dictates a relation between the magnitude and the phase of t_{QD} :

$$\mathbf{T}_{QD} = \gamma_D^2 \sin^2 \alpha_{QD}. \quad (5)$$

Without interactions,

$$G_{up} = 1/[\epsilon_k - \epsilon_d - \Sigma_0], \quad (6)$$

with the self-energy $\Sigma_0(\epsilon_k)$ depending on details of the leads connected to the QD.

3. The closed ABI

In Ref. [16], we used the equation-of-motion method to calculate the transmission amplitude through the closed ABI, t , for a simple version of Fig. 1: $n_l = n_r = 0$, $n_0 = 1$. We ended up with the result

$$t = A_D t_{QD} e^{i\phi} + A_B t_B, \quad (7)$$

where t_B was the “bare” transmission amplitude through the lower “reference” path, when the upper path was disconnected, and the coefficients A_D and A_B contain all the additional processes in which the electron “visits” the reference site (denoted 0 in the figure), or the dot, respectively. Without interactions, we were able to prove that the ϕ -dependence of \mathbf{T} has the form

$$\mathbf{T} = \mathbf{C} \frac{1 + K^2 + 2K \cos \phi}{1 + 2P(z + \cos \phi) + Q(z + \cos \phi)^2}, \quad (8)$$

where the five coefficients \mathbf{C} , K , P , Q and z are all real, and independent of ϕ . These parameters do depend explicitly on both the real and imaginary parts of G_{QD} . Although the numerator in Eq. (8) looks like the 2-slit formula, with $\beta = 0$ or π (depending on sign K), the new physics, related to the many “trips” of the electron around the ring, is contained in the denominator. Note that Eq. (8) obeys the “phase rigidity”, and also requires many harmonics in the flux. A 5-parameter fit to the explicit ϕ -dependence in Eq. (8) for given values of V_G and of the other ABI parameters then allows one to extract the V_G -dependence of G_{QD} .

Reference [16] also contained some speculations on how to use Eq. (8) in the presence of interactions, when the corrections to the self-energy due to the lower branch can be expanded in a Fourier series in ϕ , and when this series is dominated by the first harmonic (thus renormalizing the parameter z above). More recently we generalized Eq. (8) to the strongly correlated Kondo case [17]. Deep inside the Kondo regime, when the QD is occupied by a single electron, the Fermi liquid conditions constrain the Green function on the QD. The resulting Green function then depends only on the *non-interacting* self-energy $\Sigma_0(\epsilon_k)$ [see Eq. (6)]. This allowed us to obtain the exact dependence of the conductance through the ABI on the flux ϕ ,

$$\mathbf{G} = \frac{A + B \cos \phi + C \cos^2 \phi}{1 + D \cos \phi + E \cos^2 \phi}. \quad (9)$$

In this limit ($T \rightarrow 0$, $\epsilon_d \rightarrow -\infty$, $U \rightarrow \infty$), all the coefficients depend only on the non-interacting parts of the ABI. This conductance reaches the unitarity limit $2e^2/h$ for some fluxes ϕ , but its dependence on ϕ contains a non-trivial structure which is specific to the particular geometry, and not to the physics of the QD itself. Using a recently derived approximate solution for the Green function in the Kondo regime, for $U \rightarrow \infty$

[19], we found that Eq. (9) presents an excellent fit to the “data” for all ϵ_d and $T \ll T_K$. Fits to such data again allow the extraction of the Green function on the dot from the closed ABI data, also in the Kondo regime.

4. The open ABI

Imitating the experiments of Schuster *et al.* [10], we introduce the opening of the ABI via the side branches which are attached to all the sites on the ring except the QD. The algebra remains similar to the case of the closed ABI, except that various sites now have a complex self-energy, due to the side branches. Since the data were taken in the Coulomb blockade, each resonance can be imitated by a separate level on the QD, with the Coulomb interaction representing the distance between such levels. For the non-interacting case, we again end up with an equation like (8), except that the numerator is now replaced by $|1 + Ke^{i\phi}|^2$, and K is now a *complex number*. Thus, the numerator assumes the form $1 + |K|^2 + 2\Re[K e^{i\phi}]$, similar to the 2-slit Eq. (1). However, the coefficients, as well as the imaginary part of K , depend on the parameter J_X which is a measure for the opening. In Ref. [11] we fitted these calculated results to the 2-slit formula (1), and discovered that the “measured” phase β reproduces the correct phase α_{QD} only when the structure of the ABI and of the side branches are optimized: to have $\beta = \alpha_{QD}$, the electron must cross each branch only once, with no reflections anywhere. One necessary condition for this was appreciated qualitatively in an earlier publication [20]: the electron must practically never be reflected from the “forks” where the ring meets the incoming and outgoing leads. A second condition requires that the electron also passes through the QD only once, and does not “reverberate” back and forth between the “combs” on its two sides. In our model, both conditions are achieved by having a very small net transmission through *and* a very small reflection from each “comb” of “lossy” channels. As J_X increases, the transmission through the “lossy” scatterers decreases, but the reflection from them increases. Therefore, there is only an *intermediate* range of J_X where $\beta = \alpha_{QD}$.

In principle, experimentalists should vary the strength of the coupling to the side “lossy” branches,

in search for the optimal intermediate range. However, at the moment we only have the data published in Ref. [10], taken from a single realization of the open ABI. We now present two criteria which can check the consistency of the two-slit conditions in these experiments. One such criterion follows from Eq. (2), which requires that

$$b \equiv \left(\frac{B}{\max[B]} \right)^2 = |t_1|^2 = \frac{A - \min[A]}{\max[A] - \min[A]} \equiv a. \quad (10)$$

A second criterion follows from Eq. (5):

$$a = b = |t_1|^2 = \gamma_D^2 \sin(\alpha_{QD}) = \gamma_D^2 \sin^2 \beta. \quad (11)$$

Taking the data for A , B and β from the graphs of Ref. [10], we check these criteria in Fig. 2. We adjusted the scale of b arbitrarily, to optimize the fit between the curves. The reader can now judge if the data obey these criteria. At least over some energy range, and remembering the uncertainties, the data may be reasonably consistent with the two-slit requirements. However, a systematic study of open ABI’s is still desired.

More recently, we have also analyzed the open ABI for strongly correlated dots [17]. Similar to the closed case, deep inside the Kondo regime the numerator in Eq. (9) is now replaced by $A + B \cos(\phi + \beta) + C \cos(2\phi + \gamma)$, with the parameters depending only on the non-interacting parts. Thus, β depends strongly on these parts of the ABI, and experiments may end up with arbitrary values of this “measured” phase, instead of the Kondo value of $\alpha_{QD} = \pi/2$. This may explain the unexplained observations in Ref. [14]. Furthermore, we find that T_K depends strongly on the flux and on J_X , and therefore the opening of the ABI may in fact destroy the Kondo correlations on the QD and eliminate the Kondo regime altogether. Thus, the measurements in the Kondo regime are much more sensitive to the details of the ABI, compared to the non-interacting case.

5. Concluding remarks

Our main conclusion is that opening the ABI introduces many undesired uncertainties into the analysis of the data. It also reduces the outgoing current, due to the losses on the side branches. In contrast, we now have a reasonable quantitative understanding of the conductance through the closed ABI. It would there-

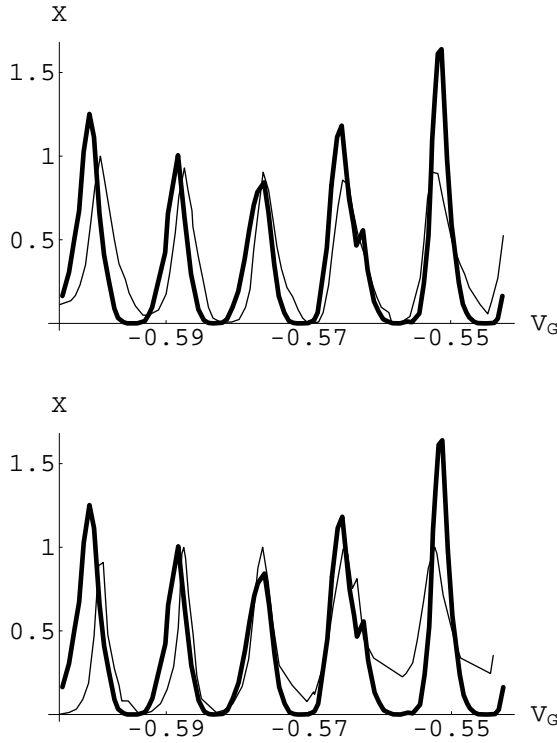


Fig. 2. Tests of Eqs. (10) (11). The thick lines represent b (rescaled arbitrariness), while the thin lines represent a (top panel) and $\sin^2[\pi(\beta - .03)]$ (the data in Ref. [10] give β in units of π).

fore be useful to have new systematic experimental studies of closed ABI's, which could test our various quantitative predictions.

Acknowledgements

We thank B. I. Halperin, Y. Meir and A. Schiller for helpful conversations. This project was carried out in a center of excellence supported by the Israel Science Foundation (under grant #1566/04), with additional support from the Albert Einstein Minerva Center for Theoretical Physics at the Weizmann Institute of Science, and from the German Federal Ministry of Education and Research (BMBF) within the Framework of the German-Israeli Project Cooperation (DIP). Work at Argonne supported by the U. S. department of energy, Basic Energy Sciences–Materials Sciences, under contract #W-31-109-ENG-38.

References

- [1] L. P. Kouwenhoven *et al.*, Mesoscopic Electron Transport, NATO Advanced Study Institute, Series E: Applied Science, Vol. **345**, edited by L. L. Sohn, L. P. Kouwenhoven and G. Schön (Kluwer, Dordrecht, 1997), p. 105.
- [2] Y. Imry, Introduction to Mesoscopic Physics (Oxford University Press, Oxford 1997; 2nd edition, 2002).
- [3] M. A. Kastner, Physics Today **46**(1) (1993) 24.
- [4] e. g. R. P. Feynmann, R. B. Leighton and M. Sands, The Feynmann Lectures on Physics, Vol. III, Chap. 1 (Addison-Wesley, Reading 1970).
- [5] Y. Gefen, Y. Imry and M. Ya. Azbel, Phys. Rev. Lett. **52** (1984) 129.
- [6] Y. Aharonov and D. Bohm, Phys. Rev. **115** (1959) 485.
- [7] A. Yacoby, M. Heiblum, D. Mahalu and H. Shtrikman, Phys. Rev. Lett. **74** (1995) 4047.
- [8] L. Onsager, Phys. Rev. **38** (1931) 2265; H. B. G. Casimir, Rev. Mod. Phys. **17** (1945) 343.
- [9] M. Büttiker, Phys. Rev. Lett. **57** (1986) 1761.
- [10] R. Schuster *et al.*, Nature **385** (1997) 417.
- [11] A. Aharony, O. Entin-Wohlman, B. I. Halperin and Y. Imry, Phys. Rev. **B66** (2002) 115311.
- [12] A. C. Hewson, The Kondo Problem for heavy Fermions (cambridge University Press, cambridge, 1993).
- [13] W. G. van der Wiel, S. De Franceschi, T. Fujisawa, J. M. Elzerman, S. Tarucha, and L. P. Kouwenhoven, Science **289** (2000) 2105.
- [14] Y. Ji, M. Heiblum, D. Sprinzak, D. Mahalu, and H. Shtrikman, Science **290** (2000) 779; Y. Ji, M. Heiblum, and H. Shtrikman, Phys. Rev. Lett. **88** (2002) 076601.
- [15] T. K. Ng and P. A. Lee, Phys. Rev. Lett. **61** (1988) 1768.
- [16] A. Aharony, O. Entin-Wohlman and Y. Imry, Phys. Rev. Lett. **90** (2003) 156802.
- [17] A. Aharony and O. Entin-Wohlman, unpublished.
- [18] N. E. Bickers, Rev. Mod. Phys. **69** (1987) 845, Table IX.
- [19] O. Entin-Wohlman, A. Aharony and Y. Meir, Phys. Rev. B (in press); cond-mat/0406453.
- [20] O. Entin-Wohlman, A. Aharony, Y. Imry, Y. Levinson and A. Schiller, Phys. Rev. Lett. **88** (2002) 166801.